universe

IMPACT FACTOR 2.5

CITESCORE 4.3

Article

Two-Loop Corrections in Power Spectrum in Models of Inflation with Primordial Black Hole Formation

Hassan Firouzjahi

Special Issue
Primordial Black Holes from Inflation

Edited by
Prof. Dr. Cristiano Germani

MDPI

https://doi.org/10.3390/universe10120456

universe

MDPI

Article

Two-Loop Corrections in Power Spectrum in Models of Inflation with Primordial Black Hole Formation

Hassan Firouzjahi

School of Astronomy, Institute for Research in Fundamental Sciences (IPM), Tehran P.O. Box 19395-5746, Iran; firouz@ipm.ir

Abstract: We calculated the two-loop corrections in the primordial power spectrum in models of single-field inflation incorporating an intermediate USR phase employed for PBH formation. Among the overall eleven one-particle irreducible Feynman diagrams, we calculated the corrections from the "double scoop" two-loop diagram involving two vertices of quartic Hamiltonians. We demonstrate herein the fractional two-loop correction in power spectrum scales, like the square of the fractional one-loop correction. We confirm our previous findings that the loop corrections become arbitrarily large in the setup where the transition from the intermediate USR to the final slow-roll phase is very sharp. This suggests that in order for the analysis to be under perturbative control against loop corrections, one requires a mild transition with a long enough relaxation period towards the final attractor phase.

Keywords: inflation; primordial black holes; loop corrections

Citation: Firouzjahi, H. Two-Loop Corrections in Power Spectrum in Models of Inflation with Primordial Black Hole Formation. *Universe* **2024**, *10*, 456. https://doi.org/10.3390/universe10120456

Academic Editor: Cristiano Germani

Received: 15 November 2024
Revised: 9 December 2024
Accepted: 12 December 2024
Published: 13 December 2024

1. Introduction

There have been intense debates in the recent literature on the nature of loop corrections in single-field models of inflation involving an intermediate ultra slow-roll (USR) phase [1–37]; for earlier works concerning the quantum loop effects in models of inflation, see [38–42]. These models have been employed to generate primordial black holes (PBHs) as candidates for the observed dark matter [43–46]; for a review on the mechanism of generating PBHs from a USR setup, see [47–51]. In the USR setup involving a flat potential, the curvature perturbation grows on superhorizon scales. The enhancement in the power spectrum allows one to use this setup to generate PBHs on desired scales. However, the rapid growth of the power spectrum during the intermediate USR stage can be problematic. More specifically, Kristiano and Yokoyama argued in [1] that the one-loop corrections originating from the small-scale USR modes can affect the CMB perturbations. Correspondingly, it was originally concluded in [1] that the analysis is not under perturbative control and the setup is not trusted for PBH formation. Following [1], the one-loop corrections in the curvature perturbation power spectrum were studied with different (conflicting) conclusions. For example, the results of [1] was criticized by Riotto [3,4], arguing that the one-loop corrections can be small if the transition to the final attractor phase is smooth enough. Similarly, in [13], employing δN formalism, it was argued that the large loop effects in the models with mild transitions are suppressed by the slow-roll parameters and the model is under perturbative control for generating PBHs. In addition, the loop corrections were studied numerically in [27] and also by employing the formalism of separate universe in [28].

In order to estimate the total one-loop corrections in the power spectrum, we need to have both the cubic and quartic Hamiltonians. The cubic action was calculated originally by Maldacena [52], but there is still no concrete result for the full quartic interaction including the USR phase; for earlier studies on quartic action, however, see [53,54]. In [11], we employed the formalism of the effective field theory (EFT) of inflation, which enabled us to calculate the cubic and the quartic Hamiltonians in reasonable ease in the decoupling limit.

Furthermore, we were able to incorporate the effects of the sharpness of the transition from the USR stage to the final slow-roll phase as well. We showed in [11] that the one-loop corrections can be dangerous in models with a sharp transition, supporting the conclusion of [1].

Based on the physical intuitions and the expectation of the decoupling of scales, it looks counterintuitive that the small USR modes can affect the long CMB scales in the first place [4,25]. Motivated by this question, the conclusion of [1] was critically revisited in [23,24], where it was claimed that the one-loop corrections are canceled. Specifically, in [23], the contributions of the boundary terms, which were not taken into account in previous works, were highlighted. On the other hand, it was argued in [24] that the loop contributions vanish after the UV limit of the momentum is considered via some $i\varepsilon$ prescription. However, in both [23,24], like many other previous works, only the cubic interactions were considered. The conclusions of [23,24] were reviewed critically in [25], highlighting the flaws in their arguments. More recently, there were new claims of loop cancellation in [55–57]; we would like to return to the results of these claims elsewhere.

As for the physical origins of the loop corrections, the non-linear coupling between the short and long modes induces a source term in the equation governing the evolution of the long mode. At the same time, the spectrum of the short modes are modulated by the long modes. The modulation effects becomes large if the power spectrum of the short modes is highly scale-dependent which is the case in the USR model. The combined effects of the non-linear coupling between the short and long modes and the modulation of the short modes by the long mode backreacts on the long mode itself, causing loop corrections, as highlighted in [3,15,25].

In light of the above discussions, in this work, we aim to calculate the corrections in power spectrum at the two-loop order. As one may expect, the analysis at two-loop order are significantly more complicated than in the one-loop case. First, we have more Feynman diagrams involving not only the cubic and quartic interactions, but also the quintic and sextic Hamiltonians. Secondly, most of these Feynman diagrams involve double- or higher-order nested in-in integrals, which make the time integral very complicated. As we shall see, there are in total eleven one-particle irreducible Feynman diagrams at the two-loop level. Out of these eleven diagrams, we consider the case of the "double scoop" diagram, which involves a double nested time integral containing two quartic Hamiltonians. We believe that the results from this case are illustrative enough, which can shed light on the structure of the two-loop corrections.

2. The Setup

In this section, we briefly review our setup. This is the same setup as employed in [1] for PBH formation. It is a single-field inflation with three distinct phases, $SR \to USR \to SR$, where the first and and the third stages are assumed to be in SR phases while the USR phase is sandwiched in between. The observed CMB perturbations leave the horizon during the first SR phase with the amplitude of power spectrum set by the COBE normalization. However, the intermediate USR phase, engineered to produce the PBHs at the desired mass scales, may start at about 30 e-folds after the CMB scales have left the Hubble horizon, and it typically lasts for 2-3 e-folds. Finally, the intermediate USR phase is followed by the second SR phase, where it is assumed that the system reaches its attractor stage.

As usual, during the SR phases, the curvature perturbation $\mathcal{R}$ is frozen after the mode leaves the horizon. However, during the USR phase, it experiences an exponential growth [58–64]. The rapid growth of the modes which become superhorizon during the intermediate USR phase is the key idea behind the enhancement in the curvature perturbation power spectrum to generate PBHs on the corresponding scales. In addition, the superhorizon growth of curvature perturbation plays important roles in violating the Maldacena non-Gaussianity consistency condition in the USR model [59–61,65–77].

Starting with the FLRW metric,

$$ds^2 = -dt^2 + a(t)^2 d\mathbf{x}^2\,, \tag{1}$$

the equations governing the dynamics of the background inflaton field ϕ and the scale factor $a(t)$ during the USR stage are

$$\ddot{\phi}(t) + 3H\dot{\phi}(t) = 0\,, \qquad 3M_P^2 H^2 \simeq V_0, \tag{2}$$

in which M_P is the reduced Planck mass, H is the Hubble expansion rate, and V_0 is the constant potential during the USR stage.

Since H is very nearly constant during the USR phase, then $\dot{\phi} \propto a^{-3}$. Correspondingly, the first slow-roll parameter $\epsilon \equiv -\frac{\dot{H}}{H^2}$ falls off like a^{-6}, while the second slow-roll parameter $\eta \equiv \frac{\dot{\epsilon}}{H\epsilon}$ is nearly constant, $\eta \simeq -6$. It is assumed that the USR phase is extended in the interval $\tau_s < \tau < \tau_e$, so ϵ, at the time of the end of the USR, is given by $\epsilon_e = \epsilon_i \left(\frac{\tau_e}{\tau_s}\right)^6$, where ϵ_i is the value of ϵ at the start of the USR phase. Here, τ is the conformal time, which is related to cosmic time as usual via $d\tau = dt/a(t)$, with the understanding that towards the end of inflation, $\tau \to 0$. Alternatively, working with the number of e-fold $dN = Hdt$ as the clock, the duration of the USR is determined by $\Delta N \equiv N(\tau_e) - N(\tau_s)$, yielding $\epsilon_e = \epsilon_i e^{-6\Delta N}$. For PBH formation, we typically require ΔN to be around 2 to 3 e-folds.

To simplify the analysis, we assume that the transitions $SR \to USR$ and $USR \to SR$ happen instantaneously, at $\tau = \tau_s$ and $\tau = \tau_e$, respectively. However, it may take time to end up in its attractor phase during the final SR phase. This is determined by the sharpness (which is actually the relaxation) parameter h, initially defined in [77] via

$$h = -6\sqrt{\frac{\epsilon_V}{\epsilon_e}}\,, \tag{3}$$

in which ϵ_V is the value of ϵ during the final slow-roll phase, which is determined as usual by the first derivative of the potential. Note that by construction, $h < 0$. In our analysis, we assume a sharp enough transition, so $|h| > 1$. For a mild transition, e.g., h, at the order of slow-roll parameters, the mode function keeps evolving during the final phase and the analysis become complicated. However, for a sharp transition, the system reaches the attractor phase quickly and the errors in our analytical results are expected to be negligible.

For a very sharp transition with $h \to -\infty$, ϵ approaches rapidly to a larger value such that towards the end of inflation, $\epsilon(\tau_0) \simeq \epsilon_V = \epsilon_e(\frac{h}{6})^2$. On the other hand, for an "instant" sharp transition, which was assumed in [1,2], one has $h = -6$. In this situation, ϵ in the third SR phase is equal to its value at the time of the end of the USR, i.e., $\epsilon_V = \epsilon_e$.

The evolution of the slow-roll parameters after the USR phase is studied in [77]. In particular, ϵ is smooth across the transition point but η experiences a jump at $\tau = \tau_e$. Prior to the transition and close to the end of the USR, $\eta = -6$, while right after the transition, we have $\eta = -6 - h$. Following [77], we can approximate η near the transition point as follows:

$$\eta = -6 - h\theta(\tau - \tau_e) \qquad \tau_e^- < \tau < \tau_e^+\,, \tag{4}$$

yielding to

$$\frac{d\eta}{d\tau} = -h\delta(\tau - \tau_e)\,, \qquad \tau_e^- < \tau < \tau_e^+\,. \tag{5}$$

As we shall see, the jump in η, highlighted by the Dirac delta function above, plays a crucial role in the loop corrections.

After presenting our background, we briefly review the perturbations in this setup. To perform the in-in analysis, we need the mode function associated to the comoving

curvature perturbation $\mathcal{R}$ during the USR and afterwards. In the Fourier space, the mode function is

$$\mathcal{R}(\mathbf{x},t) = \int \frac{d^3k}{(2\pi)^3} e^{i\mathbf{k}\cdot\mathbf{x}} \hat{\mathcal{R}}_{\mathbf{k}}(t)\,, \tag{6}$$

where, as usual, the operator $\hat{\mathcal{R}}_{\mathbf{k}}(t)$ is expressed in terms of the creation and annihilation operators $a_{\mathbf{k}}$ and $a^{\dagger}_{\mathbf{k}}$ via $\hat{\mathcal{R}}_{\mathbf{k}}(t) = \mathcal{R}_k(t)a_{\mathbf{k}} + \mathcal{R}^*_k(t)a^{\dagger}_{-\mathbf{k}}$. In this notation, $\hat{\mathcal{R}}_{\mathbf{k}}$ is a quantum operator and $\mathcal{R}_k$ is the mode function. As usual, the creation and annihilation operators satisfy the standard commutation relations $[a_{\mathbf{k}}, a^{\dagger}_{\mathbf{k}'}] = (2\pi)^3\delta(\mathbf{k}-\mathbf{k}')$.

The quantum initial condition is fixed by the Bunch–Davies vacuum with the mode function

$$\mathcal{R}^{(1)}_k = \frac{H}{M_P\sqrt{4\epsilon_i k^3}}(1+ik\tau)e^{-ik\tau}\,, \qquad (\tau<\tau_s)\,. \tag{7}$$

During the intermediate USR phase, the mode function is parameterized via

$$\mathcal{R}^{(2)}_k = \frac{H}{M_P\sqrt{4\epsilon_i k^3}}\left(\frac{\tau_s}{\tau}\right)^3\left[\alpha^{(2)}_k(1+ik\tau)e^{-ik\tau} + \beta^{(2)}_k(1-ik\tau)e^{ik\tau}\right], \tag{8}$$

in which the coefficients $\alpha^{(2)}_k$ and $\beta^{(2)}_k$ are determined by imposing the continuity of the mode function and its time derivative at $\tau=\tau_s$, yielding

$$\alpha^{(2)}_k = 1 + \frac{3i}{2k^3\tau_s^3}(1+k^2\tau_s^2)\,, \qquad \beta^{(2)}_k = -\frac{3i}{2k^3\tau_s^3}(1+ik\tau_s)^2e^{-2ik\tau_s}\,. \tag{9}$$

On the other hand, imposing the matching conditions at τ_e, the outgoing mode function during the final SR phase is given by [11]

$$\mathcal{R}^{(3)}_k = \frac{H}{M_P\sqrt{4\epsilon(\tau)k^3}}\left[\alpha^{(3)}_k(1+ik\tau)e^{-ik\tau} + \beta^{(3)}_k(1-ik\tau)e^{ik\tau}\right], \tag{10}$$

in which $\alpha^{(3)}_k$ and $\beta^{(3)}_k$ are determined to be

$$\alpha^{(3)}_k = \frac{1}{8k^6\tau_s^3\tau_e^3}\Big[3h(1-ik\tau_e)^2(1+ik\tau_s)^2e^{2ik(\tau_e-\tau_s)} - i(2k^3\tau_s^3+3ik^2\tau_s^2+3i)(4ik^3\tau_e^3-hk^2\tau_e^2-h)\Big],$$

and

$$\beta^{(3)}_k = \frac{-1}{8k^6\tau_s^3\tau_e^3}\Big[3(1+ik\tau_s)^2(h+hk^2\tau_e^2+4ik^3\tau_e^3)e^{-2ik\tau_s} + ih(1+ik\tau_e)^2(3i+3ik^2\tau_s^2+2k^3\tau_s^3)e^{-2ik\tau_e}\Big].$$

With the mode functions given above, we can calculate the two-loop corrections in the curvature perturbations' power spectrum. We choose the convention that the momentum associated to the long CMB modes are denoted by $\mathbf{p}_1$ and $\mathbf{p}_2$, while the momentum corresponding to the short modes that run inside the loops are denoted by $\mathbf{q}$ and $\mathbf{k}$. There is the vast hierarchy $p_i \ll q,k$. In our analysis, we are interested in the loop corrections induced from the short modes, which become superhorizon during the USR phase. Therefore, we cut the momentum loop integrals in the range $q_s \le q < q_e$, where $q_s = -\frac{1}{\tau_s}$ and $q_e = -\frac{1}{\tau_e}$ are the modes which leave the horizon at $\tau=\tau_s$ and $\tau=\tau_e$, respectively. Furthermore, the duration of the USR period $\Delta N \equiv N(\tau_e) - N(\tau_s)$ is given in terms of q_s and q_e by

$$e^{-\Delta N} = \frac{\tau_e}{\tau_s} = \frac{q_s}{q_e}\,. \tag{11}$$

As mentioned previously, to generate PBHs with the desired mass scales, we require $\Delta N \sim 2-3$.

In order to simplify the analysis, we have assumed an instant transition at $\tau=\tau_e$ to the final SR phase. However, the mode functions keep evolving for $\tau>\tau_e$ before it

assumes its final attractor value. This process is governed by the relaxation parameter h. For example, for an instant and sharp transition, which was employed in [1,2] with $h = -6$, at the end of inflation, $\mathcal{R}$ is smaller by a factor of $1/4$ compared to its value at $\tau = \tau_e$. The reason is that the mode function is not frozen right after the transition and it keeps evolving until it reaches its attractor value. However, for a very sharp transition corresponding to $h \to -\infty$, the mode function is assumed to freeze immediately after τ_e. This is the situation considered in [59,61], which yields $f_{NL} = \frac{5}{2}$. But, as demonstrated in [77], for a mild transition with $|h| \ll 1$, non-Gaussianity is mostly erased during the second SR phase. Motivated by these discussions, we distinguish between an instant transition and a sharp transition. For example, the assumption of an instant transition can be relaxed, and one may consider the situation where the transition takes place within some time interval [15,27]. However, this will complicate our theoretical analysis and is beyond the scope of this work.

3. Two-Loop Feynman Diagrams and Interaction Hamiltonians

In order to obtain the loop corrections in the curvature perturbation power spectrum $\mathcal{P}_\mathcal{R}$, we need the interaction Hamiltonians. Here we present the structure of two-loops Feynman diagrams and the subset of interaction Hamiltonians necessary for our two-loop calculations.

To understand the structure of Feynman diagrams associated at the two-loop level, consider a general L-loop one-particle irreducible Feynman diagram associated to the following scalar-type potential:

$$V = \sum_n g_n \phi^n \qquad (n > 2)\,, \tag{12}$$

in which g_n is the coupling (vertex) and n is the order of interaction. For example, for the cubic and quartic interactions, we have $n = 3$ and $n = 4$, respectively. Suppose that we have a Feynman diagram with L loops, P internal propagators, V_n vertices associated to each power of interaction n, and N external lines. For example, in our case of interest, $L = 2$ (two-loops) and $N = 2$ (two external lines for power spectrum). Then, using the following topological conditions [78]:

$$L = P - \sum_n V_n + 1 \tag{13}$$

and

$$N + 2P = \sum_n n V_n\,, \tag{14}$$

we obtain the following relation between L, N and V_n:

$$2L = (2 - N) + \sum_n (n-2) V_n\,. \tag{15}$$

For the loop corrections in the power spectrum with $N = 2$, this further simplifies to

$$2L = \sum_n (n-2) V_n \qquad (N = 2)\,. \tag{16}$$

In particular, for one-loop corrections, the above condition allows for only two Feynman diagrams, a single quartic vertex, and a diagram with two cubic vertices, as studied in detail in [11].

Now, in our current case of interest with two-loop corrections ($L = 2$), Equation (16) yields the following constraint:

$$4 = V_3 + 2V_4 + 3V_5 + 4V_6\,. \tag{17}$$

Based on the allowed integer solutions of the above equation, one obtains the allowed Feynman diagrams. Below are all possible allowed solutions:

$$\begin{aligned}
&(1) \quad : V_6 = V_5 = V_3 = 0,\ V_4 = 2\,,\\
&(2) \quad : V_6 = V_5 = V_4 = 0,\ V_3 = 4,\\
&(3) \quad : V_6 = V_5 = 0,\ V_4 = 1, V_3 = 2,\\
&(4) \quad : V_6 = V_4 = 0,\ V_3 = V_5 = 1\,,\\
&(5) \quad : V_3 = V_4 = V_5 = 0,\ V_6 = 1\,.
\end{aligned} \tag{18}$$

The above solutions yield 11 distinct two-loop diagrams as plotted in Figure 1. The Feynman diagrams in the first category involves two vertices of quartic Hamiltonian $\mathbf{H}_4$ (diagrams (**a**,**b**) in Figure 1), while the diagrams in the second category involve four vertices of the cubic Hamiltonian $\mathbf{H}_3$ (diagrams (**c**,**d**)). The diagrams in the third category contain three vertices, one from $\mathbf{H}_4$ and two from $\mathbf{H}_3$ (diagrams (**e**–**h**)). On the other hand, the diagram in the fourth category involves two vertices, one from $\mathbf{H}_3$ and one from the quintic interaction $\mathbf{H_5}$ (diagrams (**k**,**l**)). Finally, the diagram in the fifth category involves a single vertex from the sextic Hamiltonian $\mathbf{H_6}$ (diagram (**m**)). From the above discussions, we see that we need $\mathbf{H}_3, \mathbf{H}_4, \mathbf{H}_5$ and $\mathbf{H}_6$ to calculate the full two-loop corrections in $\mathcal{P}_\mathcal{R}$.

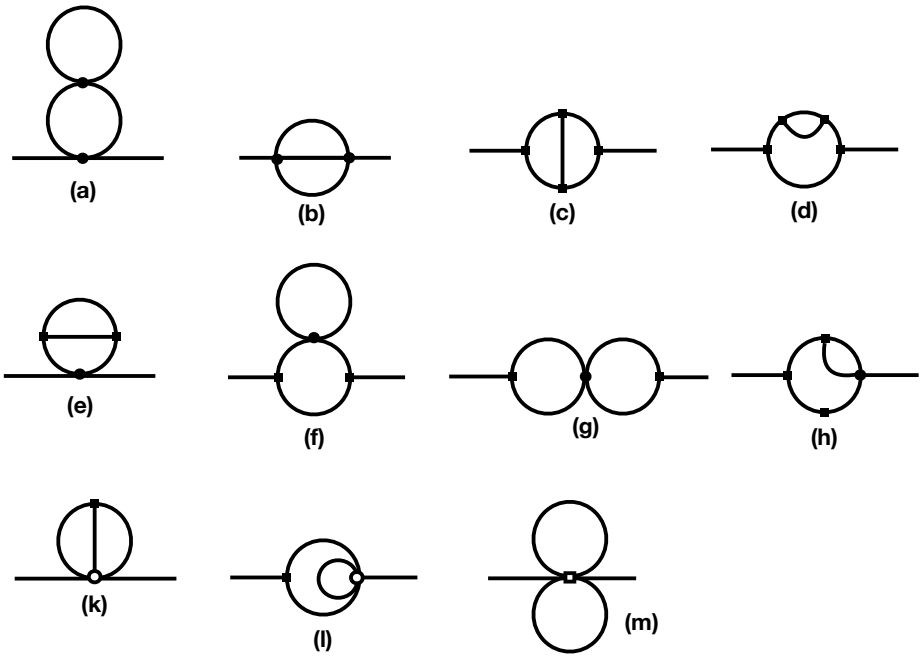

Figure 1. The one-particle irreducible Feynman diagrams for the two-loop corrections constructed from the solutions of Equation (18). The diagrams (**a**,**b**) belong to category (1) in Equation (18), diagrams (**c**,**d**) to category (2), diagrams (**e**–**h**) to category (3), diagrams (**k**,**l**) belong to categories (4), and diagram (**m**) belongs to category (5).

The cubic action for the curvature perturbations $\mathcal{R}$ and the corresponding cubic Hamiltonian were calculated in detail by Maldacena [52]. However, calculating the quartic action and the corresponding quartic Hamiltonian in this method is a very difficult task. Fortunately, the formalism of the EFT of inflation [79,80] provides a very useful alternative, in which the interaction Hamiltonians can be calculated with reasonable ease. In particular, in the decoupling limit where the gravitational backreactions can be neglected, the EFT formalism was employed to calculate the cubic and quartic Hamiltonians in [11] (see also [66] for the first work in this direction, calculating the cubic Hamiltonian). While the

cubic and the quartic Hamiltonians were constructed in [11], one still needs to calculate $\mathbf{H}_5$ and $\mathbf{H}_6$ to perform the full two-loop corrections. In principle, it is possible to calculate $\mathbf{H}_5$ and $\mathbf{H}_6$ using the EFT approach, but it turns out that there are new technical complications which require careful considerations [81].

The analysis of full two-loop corrections associated to the above 11 diagrams is a demanding task. As a first step forward, we calculated the two-loop corrections from the "double scoop" diagram (**a**), which are relatively easier to technically handle. This is because this diagram involves two vertices, so one deals with double nested in-in integrals (this is also true for diagram (**b**)). However, diagrams (**c**–**h**) contain nested integrals with three-fold or four-fold time integrals involving $\mathbf{H}_3$ or $\mathbf{H}_4$, which are far more complicated than diagram (**a**). As we shall see, the analysis even for the simple-looking diagram (**a**) is non-trivial. Having said this, physically, one expects that the result obtained from this single diagram will shed light onto the structure of two-loop corrections, which should not be vary different than the remaining diagrams.

Here, we briefly review the results of [11], which are required to calculate the quartic Hamiltonian to calculate the loop corrections from diagram (**a**). We refer the reader to [11] for further details.

The second-order action employed to quantize the free theory is

$$S_2 = M_P^2 \int d\tau d^3x\, a^2 \epsilon H^2 \left(\pi'^2 - (\partial_i \pi)^2\right), \tag{19}$$

in which the prime represents the derivative with respect to τ. Here, $\pi(x^\mu)$ is the Goldstone boson associated to time diffeomorphism breaking, which is related to curvature perturbations $\mathcal{R}$ [79,80].

The cubic action is given by

$$S_{\pi^3} = M_P^2 H^3 \int d\tau d^3x\, \eta \epsilon a^2 \left[\pi \pi'^2 - \pi (\partial \pi)^2\right], \tag{20}$$

and the corresponding cubic interaction Hamiltonian is given by [66]

$$\mathbf{H}_3 = -M_P^2 H^3 \eta \epsilon a^2 \int d^3x \left[\pi \pi'^2 + \frac{1}{2}\pi^2 \partial^2 \pi\right]. \tag{21}$$

On the other hand, the quartic action is obtained to be

$$S_{\pi^4} = \frac{M_P^2}{2} \int d\tau d^3x\, \epsilon a H^3 \left(\eta^2 a H + \eta'\right) \left[\pi^2 \pi'^2 - \pi^2 (\partial \pi)^2\right]. \tag{22}$$

In particular, note that there is the term η', which induces the delta contribution $\delta(\tau - \tau_e)$ in the interaction Hamiltonian when η undergoes a jump at $\tau = \tau_e$, as given by Equation (5).

As discussed in [11], in calculating the quartic Hamiltonian, care must be taken as the time derivative interaction $\pi' \pi^2$ in $\mathbf{H}_3$ induces an additional contribution in the quartic Hamiltonian [82,83]. As a result, one can not simply conclude that $\mathbf{H}_4 = -\mathbf{L}_4$. More specifically, the quartic Hamiltonian receives additional contribution $+M_P^2 H^4 \eta^2 \epsilon a^2\, \pi^2 \pi'^2$ from the cubic action. Combining all contributions, the total quartic Hamiltonian is given by [11]

$$\mathbf{H}_4 = \frac{M_P^2}{2} \epsilon a H^3 \int d^3x \left[\left(\eta^2 a H - \eta'\right) \pi^2 \pi'^2 + \left(\eta^2 a H + \eta'\right) \pi^2 (\partial \pi)^2\right]. \tag{23}$$

The interaction Hamiltonians (21) and (23) have been used in [11] to calculate the one-loop corrections to the power spectrum. We note that in obtaining the above Hamiltonian, we have ignored total time derivatives in the form $\frac{d}{dt}\left(f(t)\pi^4\right)$, where $f(t)$ is a function of the background quantity. However, as shown in [33], these boundary terms are harmless as they do not involve $\dot{\pi}$ and their contributions can be absorbed via a canonical transformation in phase space.

The quantity of interest is the curvature perturbation $\mathcal{R}$, while the above interaction Hamiltonians are given in terms of the Goldstone field π. The relation between $\mathcal{R}$ and π is non-linear. For example, to cubic order in π, they are related to each other via [53,54]

$$\begin{aligned}\mathcal{R} &= -H\pi + \big(H\pi\dot{\pi} + \frac{\dot{H}}{2}\pi^2\big) + \big(-H\pi\dot{\pi}^2 - \frac{H}{2}\ddot{\pi}\pi^2 - \dot{H}\dot{\pi}\pi^2 - \frac{\ddot{H}}{6}\pi^3\big)\,,\\ &= -H\pi + \frac{1}{2}\frac{d}{dt}\big(H\pi^2\big) - \frac{1}{6}\frac{d^2}{dt^2}\big(H\pi^3\big)\,. \end{aligned} \tag{24}$$

However, we calculate the loop corrections in power spectrum at the time of end of inflation $\tau = \tau_0 \to 0$ when it is assumed that the system is in the slow-roll phase and the long mode perturbations are frozen with $\dot{\pi} = \ddot{\pi} = 0$. Fortunately, one can neglect the non-linear corrections in $\mathcal{R}$ in Equation (24) in this limit and simply consider the linear relation between them,

$$\mathcal{R} = -H\pi\,, \qquad (\tau \to \tau_0). \tag{25}$$

Since the relation between $\mathcal{R}$ and π is linear at τ_0, we can simply write $\langle\mathcal{R}(\tau_0)\mathcal{R}(\tau_0)\rangle = H^2\langle\pi(\tau_0)\pi(\tau_0)\rangle$. Consequently, one can use π and $\mathcal{R}$ interchangeably in the following in-in analysis. More specifically, we will use the free mode function of $\mathcal{R}$ in the interaction picture in place of the π perturbations in the following in-in integrals.

4. Loop Corrections in Power Spectrum

Employing the perturbative in-in formalism [84], the expectation value of the quantum operator $\hat{O}[\tau_0]$ measured at the time of end of inflation τ_0 is,

$$\langle\hat{O}(\tau_0)\rangle = \Big\langle\Big[\bar{\mathrm{T}}\exp\Big(i\int_{-\infty}^{\tau_0}d\tau' H_{\rm in}(\tau')\Big)\Big]\,\hat{O}(\tau_0)\,\Big[\mathrm{T}\exp\Big(-i\int_{-\infty}^{\tau_0}d\tau' H_{\rm in}(\tau')\Big)\Big]\Big\rangle\,. \tag{26}$$

Here, as usual, T and $\bar{\mathrm{T}}$ represent the time ordering and anti-time ordering respectively and $H_{\rm in}(t)$ is the interaction Hamiltonian. For our case of interest here $\hat{O}(\tau_0) = \mathcal{R}_{\mathbf{p}_1}(\tau_0)\mathcal{R}_{\mathbf{p}_2}(\tau_0)$, while for the Feynman diagram (**a**) which we consider, we only need the quartic interactions so $H_{\rm in} = \mathbf{H}_4$.

In order to calculate the two-loop corrections, one requires to expand the in-in formula Equation (26) to second orders $H_{\rm in}$. For this purpose, it is more convenient to use the Weinberg commutator method associated to Equation (26). To the second order in $H_{\rm in} = \mathbf{H}_4$, we obtain [84],

$$\langle\hat{O}(\tau_0)\rangle = i^2\int_{-\infty}^{\tau_0}d\tau_2\int_{-\infty}^{\tau_2}d\tau_1\Big\langle\Big[H_{\rm in}(\tau_1),\big[H_{\rm in}(\tau_2),\hat{O}(\tau_0)\big]\Big]\Big\rangle \tag{27}$$

$$= 2\int_{-\infty}^{\tau_0}d\tau_2\int_{-\infty}^{\tau_2}d\tau_1\mathrm{Re}\Big[\big\langle\mathbf{H_4}(\tau_1)\hat{O}(\tau_0)\mathbf{H_4}(\tau_2)\big\rangle - \big\langle\mathbf{H_4}(\tau_1)\mathbf{H_4}(\tau_2)\hat{O}(\tau_0)\big\rangle\Big]\,, \tag{28}$$

with $\hat{O}(\tau_0) \equiv \mathcal{R}_{\mathbf{p}_1}(\tau_0)\mathcal{R}_{\mathbf{p}_2}(\tau_0)$.

Depending on the contractions of external leg operators $\hat{O}(\tau_0)$, there are two distinct Feynman diagrams as shown by diagrams (**a**) and (**b**) in Figure 1. The diagram (**a**) corresponds to the situation in which $\hat{O}(\tau_0)$ contracts only with $\mathbf{H_4}(\tau_2)$, with no contractions to $\mathbf{H_4}(\tau_1)$. On the other hand, the diagram (**b**) corresponds to the case where $\hat{O}(\tau_0)$ contracts jointly with both $\mathbf{H_4}(\tau_2)$ and $\mathbf{H_4}(\tau_1)$. AS mentioned before, as a first try for the two-loop corrections, in this work, we only consider the "double scoop" diagram (**a**).

It turns out that it is very convenient to decompose the expectation values in terms of sub-component Wick contractions. As an example, consider $\big\langle\mathbf{H_4}(\tau_1)\hat{O}(\tau_0)\mathbf{H_4}(\tau_2)\big\rangle$ in the second line in Equation (28). It involves three forms of contractions: $\overbrace{\mathbf{H_4}(\tau_1)\mathbf{H_4}(\tau_2)}$, $\overbrace{\hat{O}(\tau_0)\mathbf{H_4}(\tau_2)}$, and $\overbrace{\mathbf{H_4}(\tau_1)\mathbf{H_4}(\tau_1)}$. Let us define

$$\overbrace{\mathbf{H_4}(\tau_1)\mathbf{H_4}(\tau_2)} \equiv h(\tau_1,\tau_2)\,, \qquad \overbrace{\hat{O}(\tau_0)\mathbf{H_4}(\tau_2)} \equiv g(\tau_2)\,, \qquad \overbrace{\mathbf{H_4}(\tau_1)\mathbf{H_4}(\tau_1)} \equiv c(\tau_1)\,. \tag{29}$$

With these definitions, considering both terms in the second line of Equation (28), we obtain

$$\langle \hat{O}(\tau_0)\rangle = -4\int_{-\infty}^{\tau_0} d\tau_2 \int_{-\infty}^{\tau_2} d\tau_1 \mathrm{Im}[g(\tau_2)]\,\mathrm{Im}\big[c(\tau_1)h(\tau_1,\tau_2)\big]\,. \tag{30}$$

Our job is now to calculate the functions $g(\tau_2), c(\tau_1)$ and $h(\tau_1,\tau_2)$ for various possible contractions.

To perform the in-in integrals, we write $\mathbf{H_4}$ in Equation (23) as follows (neglecting the non-linear relations between π and $\mathcal{R}$ as discussed before):

$$\mathbf{H_4} = A_4(\tau)\int d^3\mathbf{x}\,\mathcal{R}^2\mathcal{R}'^2 + B_4(\tau)\int d^3\mathbf{x}\,\mathcal{R}^2(\partial\mathcal{R})^2\,, \tag{31}$$

with

$$A_4(\tau) \equiv \frac{1}{2}M_P^2\eta^2\epsilon a^2\Big(1-\frac{h}{\eta^2}\delta(\tau-\tau_e)\tau_e\Big)\,, \qquad B_4(\tau) \equiv \frac{1}{2}M_P^2\eta^2\epsilon a^2\Big(1+\frac{h}{\eta^2}\delta(\tau-\tau_e)\tau_e\Big)\,. \tag{32}$$

In particular, note the term $\delta(\tau-\tau_e)$ appearing above, which is originated from the term η' in $\mathbf{H_4}$; see Equation (5).

Depending on which term that $\mathbf{H_4}$ is contracted with each other and with $\hat{O}(\tau_0)$, we will have four different contributions, as follows:

$$\langle \hat{O}(\tau_0)\rangle = \langle \hat{O}\rangle_{A_4A_4} + \langle \hat{O}\rangle_{A_4B_4} + \langle \hat{O}\rangle_{B_4A_4} + \langle \hat{O}\rangle_{B_4B_4}\,, \tag{33}$$

For example, for $\langle \hat{O}\rangle_{A_4A_4}$, we have

$$\langle \hat{O}\rangle_{A_4A_4} = \int_{-\infty}^{\tau_0} d\tau_2 \int_{-\infty}^{\tau_2} d\tau_1 A_4(\tau_1)A_4(\tau_2)\int d^3\mathbf{x}\int d^3\mathbf{y}\Big\langle\Big[\mathcal{R}^2\mathcal{R}'^2(\mathbf{x},\tau_1),\big[\hat{O}(\tau_0),\mathcal{R}^2\mathcal{R}'^2(\mathbf{y},\tau_2)\big]\Big]\Big\rangle\,. \tag{34}$$

Proceeding to the Fourier space, this is cast into

$$\begin{aligned}\langle \hat{O}\rangle_{A_4A_4} = \int_{-\infty}^{\tau_0} d\tau_2 \int_{-\infty}^{\tau_2} d\tau_1 A_4(\tau_1)A_4(\tau_2)\Big[\prod_i^4\int\frac{d^3\mathbf{q}_i}{(2\pi)^3}(2\pi)^3\delta^3(\sum_i\mathbf{q}_i)\Big]\Big[\prod_j^4\int\frac{d^3\mathbf{k}_i}{(2\pi)^3}(2\pi)^3\delta^3(\sum_i\mathbf{k}_i)\Big]\\ \times\Big\langle\Big[(\hat{\mathcal{R}}_{\mathbf{q}_1}\hat{\mathcal{R}}_{\mathbf{q}_2}\hat{\mathcal{R}}'_{\mathbf{q}_3}\hat{\mathcal{R}}'_{\mathbf{q}_4})(\tau_1),\Big[(\hat{\mathcal{R}}_{\mathbf{p}_1}\hat{\mathcal{R}}_{\mathbf{p}_2})(\tau_0),(\hat{\mathcal{R}}_{\mathbf{k}_1}\hat{\mathcal{R}}_{\mathbf{k}_2}\hat{\mathcal{R}}'_{\mathbf{k}_3}\hat{\mathcal{R}}'_{\mathbf{k}_4})(\tau_2)\Big]\Big]\Big\rangle\,.\end{aligned} \tag{35}$$

After performing the contractions and imposing the constraints from the delta functions, in the soft limit where $p \ll q,k$, we end up with the following form of two-loop integrals

$$\big\langle\mathcal{R}_{\mathbf{p}_1}\mathcal{R}_{\mathbf{p}_2}(\tau_0)\big\rangle_{A_4A_4} = (2\pi)^3\delta^3(\mathbf{p}_1+\mathbf{p}_2)\int_{-\infty}^{\tau_0} d\tau_2\int_{-\infty}^{\tau_2} d\tau_1 A_4(\tau_1)A_4(\tau_2)\int\frac{d^3\mathbf{q}}{(2\pi)^3}\int\frac{d^3\mathbf{k}}{(2\pi)^3}F(\tau_1,\tau_2;k,q),$$

in which the function $F(\tau_1,\tau_2;k,q)$ is determined by different values of $c(\tau_1), g(\tau_2)$ and $h(\tau_1,\tau_2)$.

There are nine different terms in $F(\tau_1,\tau_2;k,q)$ from different contractions. We list them as follows:

$$\begin{aligned}&(a_0): (-4)(2)^2\mathrm{Im}\big[\mathcal{R}_p(\tau_0)^2\mathcal{R}_p^*(\tau_2)^2\big]\mathrm{Im}\big[\mathcal{R}_k{}'(\tau_1)^2\mathcal{R}_k'^*(\tau_2)^2\big]|\mathcal{R}_q(\tau_1)|^2\\ &(b_0): (-4)(2)^2\mathrm{Im}\big[\mathcal{R}_p(\tau_0)^2\mathcal{R}_p^*(\tau_2)^2\big]\mathrm{Im}\big[\mathcal{R}_k(\tau_1)^2\mathcal{R}_k'^*(\tau_2)^2\big]|\mathcal{R}'_q(\tau_1)|^2\\ &(c_0): (-4)(2)^3\mathrm{Im}\big[\mathcal{R}_p(\tau_0)^2\mathcal{R}_p^*(\tau_2)^2\big]\mathrm{Im}\big[\mathcal{R}_k(\tau_1)\mathcal{R}_k{}'(\tau_1)\mathcal{R}_k'^*(\tau_2)^2\big]\mathrm{Re}\big[\mathcal{R}_q(\tau_1)\mathcal{R}'_q(\tau_1)^*\big],\end{aligned} \tag{36}$$

and

$$
\begin{aligned}
(d_0) &: (-4)(2)^4 \mathrm{Im}\left[\mathcal{R}_p(\tau_0)^2 \mathcal{R}_p^*(\tau_2) \mathcal{R}_p'^*(\tau_2)\right] \mathrm{Im}\left[\mathcal{R}_k'(\tau_1)^2 \mathcal{R}_k'^*(\tau_2) \mathcal{R}_k^*(\tau_2)\right] |\mathcal{R}_q(\tau_1)|^2 \\
(e_0) &: (-4)(2)^4 \mathrm{Im}\left[\mathcal{R}_p(\tau_0)^2 \mathcal{R}_p^*(\tau_2) \mathcal{R}_p'^*(\tau_2)\right] \mathrm{Im}\left[\mathcal{R}_k(\tau_1)^2 \mathcal{R}_k'^*(\tau_2) \mathcal{R}_k^*(\tau_2)\right] |\mathcal{R}'_q(\tau_1)|^2 \\
(f_0) &: (-4)(2)^5 \mathrm{Im}\left[\mathcal{R}_p(\tau_0)^2 \mathcal{R}_p^*(\tau_2) \mathcal{R}_p'^*(\tau_2)\right] \mathrm{Im}\left[\mathcal{R}_k(\tau_1) \mathcal{R}_k'(\tau_1) \mathcal{R}_k'^*(\tau_2) \mathcal{R}_k^*(\tau_2)\right] \mathrm{Re}\left[\mathcal{R}_q(\tau_1) \mathcal{R}'_q(\tau_1)^*\right],
\end{aligned}
\tag{37}
$$

and

$$
\begin{aligned}
(m) &: (-4)(2)^2 \mathrm{Im}\left[\mathcal{R}_p(\tau_0)^2 \mathcal{R}_p'^*(\tau_2)^2\right] \mathrm{Im}\left[\mathcal{R}_k'(\tau_1)^2 \mathcal{R}_k^*(\tau_2)^2\right] |\mathcal{R}_q(\tau_1)|^2, \\
(n) &: (-4)(2)^2 \mathrm{Im}\left[\mathcal{R}_p(\tau_0)^2 \mathcal{R}_p'^*(\tau_2)^2\right] \mathrm{Im}\left[\mathcal{R}_k(\tau_1)^2 \mathcal{R}_k^*(\tau_2)^2\right] |\mathcal{R}'_q(\tau_1)|^2, \\
(r) &: (-4)(2)^3 \mathrm{Im}\left[\mathcal{R}_p(\tau_0)^2 \mathcal{R}_p'^*(\tau_2)^2\right] \mathrm{Im}\left[\mathcal{R}_k(\tau_1) \mathcal{R}_k'(\tau_1) \mathcal{R}_k^*(\tau_2)^2\right] \mathrm{Re}\left[\mathcal{R}_q(\tau_1) \mathcal{R}'_q(\tau_1)^*\right].
\end{aligned}
\tag{38}
$$

One subtle issue in the above expressions is the appearance of the term $\mathrm{Re}\left[\mathcal{R}_q(\tau_1) \mathcal{R}'_q(\tau_1)^*\right]$ in terms (c_0), (f_0), and (r_0). This term originates from the contraction of $\hat{\mathcal{R}}$ and $\hat{\mathcal{R}}'$ in $\mathcal{R}^2 \mathcal{R}'^2$ in $A_4(\tau_1)$. As $\hat{\mathcal{R}}$ and $\hat{\mathcal{R}}'$ do not commute, we have symmetrized the ordering of $\hat{\mathcal{R}}$ and $\hat{\mathcal{R}}'$ in $A_4(\tau_1)$, which yields $\mathrm{Re}\left[\mathcal{R}_q(\tau_1) \mathcal{R}'_q(\tau_1)^*\right]$ in terms (c_0), (f_0), and (r_0).

Looking at the above expressions, we notice that the terms containing momentum q are separated from the terms containing the momentum k. This property is depicted in Figure 2, where the momentum q runs in the top loop attached to time τ_1, while the momentum k runs in the lower loop attached to both τ_1 and τ_2. This is a simplifying feature of the diagram (**a**) in our Feynman diagrams. Because of this separation of the two momenta, it is technically easier to calculate the corrections from diagram (**a**) compared to diagram (**b**) in Figure 1. While this is a simplification, calculating the time integrals is still a non-trivial task. This is because we have two nested integrals over τ_1 and τ_2 involving 10 factors of $\mathcal{R}(\tau)$ and its derivatives.

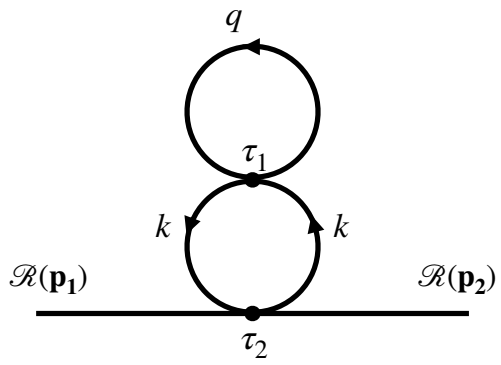

Figure 2. The arrangement of momenta inside each loop and the relative positions of τ_1 and τ_2.

The above three classes of contributions in Equations (36)–(38) are grouped by their form of the function $c(\tau_1)$, which depends only on the soft momentum p but not on the loop momenta q and k. Now, calculating these common factors in each class, we obtain

$$
\mathrm{Im}\left[\mathcal{R}_p(\tau_0)^2 \mathcal{R}_p^*(\tau_2)^2\right] = \frac{-H^4 \tau_s^6}{24 M_P^4 \epsilon_i^2 h \tau_e^3 \tau^3 p^3} \left(h \tau_e^3 + (6-h) \tau^3\right), \tag{39}
$$

$$
\mathrm{Im}\left[\mathcal{R}_p(\tau_0)^2 \mathcal{R}_p^*(\tau_2) \mathcal{R}_p'^*(\tau_2)\right] = \frac{H^4 \tau_s^6}{16 M_P^4 \epsilon_i^2 \tau^4 p^3}, \tag{40}
$$

and

$$\mathrm{Im}\left[\mathcal{R}_p(\tau_0)^2\mathcal{R}_p'^*(\tau_2)^2\right] = \frac{H^4\tau_s^6(6\tau_s^5-\tau^5)}{40M_P^4\epsilon_i^2\tau^8 p}\,. \tag{41}$$

Comparing the above three expressions, we conclude that the term in Equation (41) is much more suppressed compared to the terms in Equations (39) and (40) in the soft limit, where $p \to 0$. Correspondingly, we can neglect the contributions of the terms (m), (n) and (r) in Equation (38).

We present the details of the analysis concerning the remaining three contributions $\langle\hat{O}\rangle_{A_4B_4}$, $\langle\hat{O}\rangle_{B_4A_4}$ and $\langle\hat{O}\rangle_{B_4B_4}$ in Appendix A.

Before presenting the final result, it is useful to have an estimate of the leading contributions. Let us look at the contributions of terms (a_0) and (b_0). The difference is that in (a_0), $\mathcal{R}'$ comes with k inside the expression $\mathrm{Im}\left[\mathcal{R}_k{}'(\tau_1)^2\mathcal{R}_k'^*(\tau_2)^2\right]$, while in (b_0), $\mathcal{R}'$ involves the momentum q simply as $|\mathcal{R}'_q(\tau_1)|^2$. On the other hand, for the superhorizon perturbations during the USR phase, we have that

$$\mathcal{R}_q{}'(\tau) \simeq -\frac{3}{\tau}\mathcal{R}_q(\tau) \propto \tau^{-4}\,. \tag{42}$$

Therefore, the leading effects in the in-in integrals on the superhorizon limit where $\tau_i \to 0$ are controlled by the contributions of $\mathcal{R}'$. Since the term (b_0) involves $|\mathcal{R}'_q(\tau_1)|^2$, it scales like τ_1^{-8}, while in $\mathrm{Im}\left[\mathcal{R}_k{}'(\tau_1)^2\mathcal{R}_k'^*(\tau_2)^2\right]$, the dependence cannot be steeper than this. Indeed, calculating the leading terms on superhorizon limits of $\tau_1, \tau_2 \to 0$, one can show that the ratio $(a_0)/(b_0)$ scales like $(k\tau_1)^2$, which becomes smaller than unity on superhorizon scales. Therefore, it is expected that the contribution of the term (b_0) is more dominant than the term (a_0). Indeed, calculating the in-in integrals for both terms (a_0) and (b_0), and neglecting the numerical prefactors and the common $(2\pi)^3\delta^3(\mathbf{p}_1+\mathbf{p}_2)$, we obtain that they scale as follows:

$$(a_0) : (\mathcal{P}_{\rm CMB})^3\, e^{12\Delta N}\Delta N\,, \qquad (b_0) : (\mathcal{P}_{\rm CMB})^3\, e^{12\Delta N}\Delta N^2 \tag{43}$$

in which $\mathcal{P}_{\rm CMB}$ is the tree-level CMB scale power spectrum:

$$\mathcal{P}_{\rm CMB} = \frac{H^2}{8\pi^2\epsilon_i M_P^2}\,. \tag{44}$$

For large enough ΔN, the contributions from (b_0) is typically larger than that of (a_0), as expected.

As we demonstrated in Appendix A, in total, there are 15 leading contributions (i.e., containing p^{-3}) given by (a_0), (b_0), (c_0), (d_0), (e_0), (f_0), (a_1), (b_1), (c_1), (a_2), (b_2), (c_2), (d_2), (e_2), (f_2), (a_3), and (b_3) presented in Appendix A. The contributions from these 15 terms are either like the contribution from the (a_0) term scaling like $e^{12\Delta N}\Delta N$ or like that of the (b_0) term, scaling like $e^{12\Delta N}\Delta N^2$. It turns out that only the contributions from terms (b_0), (c_0), (d_0), (e_0) and (f_0) have the latter form.

In the limit of large enough ΔN, and adding the contributions of terms (b_0), (c_0), (d_0), (e_0), and (f_0) as the leading terms, we obtain the following fractional two-loop correction:

$$\frac{\Delta\mathcal{P}^{(2-\rm loop)}}{\mathcal{P}_{\rm CMB}} \simeq -\frac{27(23h^2+132h+1152)}{8h}\, e^{12\Delta N}\Delta N^2\mathcal{P}_{\rm CMB}^2\,, \tag{45}$$

where we have neglected the subleading terms involving $\Delta N e^{12\Delta N}$. The fact that the leading two-loop corrections scale as $e^{12\Delta N}\Delta N^2$ is both interesting and reassuring. In addition, the two-loop corrections scale linearly with h for $h \to -\infty$. Note that our result above is obtained assuming a sharp enough transition with $|h| > 1$, where the effects of the relaxation during the final SR phase are neglected.

It is instructive to compare the above two-loop corrections associated to diagram (**a**) with the full one-loop correction obtained in [11]:

$$\frac{\Delta\mathcal{P}^{(1-\text{loop})}}{\mathcal{P}_{\text{CMB}}} \simeq \frac{6(h^2+24h+180)}{h} e^{6\Delta N}\Delta N\mathcal{P}_{\text{CMB}}. \tag{46}$$

Comparing Equations (45) and (46), we obtain

$$\frac{\Delta\mathcal{P}^{(2-\text{loop})}}{\mathcal{P}_{\text{CMB}}} \sim \Big(\frac{\Delta\mathcal{P}^{(1-\text{loop})}}{\mathcal{P}_{\text{CMB}}}\Big)^2. \tag{47}$$

This is an interesting result, indicating that the fractional two-loop corrections is typically the square of the fractional one-loop correction.

For the loop effects to be under perturbative control, one requires that the successive loop corrections to be hierarchical, i.e., $\mathcal{P}_{\text{CMB}} > \Delta\mathcal{P}^{(1-\text{loop})} > \Delta\mathcal{P}^{(2-\text{loop})}$. Neglecting the numerical prefactors, from Equations (45) and (46), we obtain

$$\frac{\Delta\mathcal{P}^{(2-\text{loop})}}{\Delta\mathcal{P}^{(1-\text{loop})}} \sim \frac{\Delta\mathcal{P}^{(1-\text{loop})}}{\mathcal{P}_{\text{CMB}}} \sim e^{6\Delta N}\Delta N\mathcal{P}_{\text{CMB}}\,. \tag{48}$$

This shows that if the fractional one-loop correction is not small, then the two-loop corrections become significant as well, so the perturbative treatment quickly loses control. As elaborated in [11], the one-loop correction becomes significant for a sharp transition when $|h| \gg 1$, as can be seen in Equation (46). Therefore, we conclude that the two-loop corrections become significant in a model of sharp transition, which can be seen in Equation (45) as well. In order for the loop corrections to be under perturbative control, one has to either have a mild transition with h at the order of slow-roll parameters, or to take the duration of the USR phase to be reasonably short, e.g., $\Delta N \lesssim 1$. However, the latter arrangement may not be suitable for the PBH formation as we need a long enough period of the USR phase to enhance the power spectrum in the first place. For example, with $h = -6$, we need $\Delta N \lesssim 2.3$ to enhance $\mathcal{P}_{\mathcal{R}}$ by 7 orders of magnitudes compared to the CMB scale for the purpose of PBH formation, while still satisfying the perturbative bound from one-loop correction in Equation (46). Therefore, the only safe strategy for PBH formation in this setup is to employ a mild transition with $|h| \ll 1$.

There are two important comments in order. The first comment is that in this work, we studied the corrections from the diagram (**a**) in Figure 1. Naturally, one may ask how the two-loop corrections from the remaining ten diagram can be compared to the current result given in Equation (45). In a work in progress [81], we are studying the correction from diagram (**m**) in Figure 1 involving a single vertex of sextic Hamiltonian. We have confirmed that it scales like Equation (45). On the physical ground, we expect the full two-loop corrections to have the same general form as in Equation (45), i.e., scaling like $\Delta N^2 e^{12\Delta N}$. The second comment is the the issue of regularization and renormalization. In the current analysis, we have restricted the momentum in the range $q_s \leq q \leq k_e$. In principle, one should integrate over the entire range $q_{IR} < q < q_f$, in which q_{IR} is the lower IR limit, while q_f represents the mode which leaves the horizon at the time of the end of inflation. Alternatively, one may simply set $q_f \to \infty$. While the IR contributions are under control, the UV contribution will diverge, which has to be regularized and renormalized. Having said this, the peak of the power spectrum at the end of the USR, the dimensionless factor $e^{6\Delta N}\mathcal{P}_{\text{CMB}}$ fixes the overall scale of the finite term after regularization. The fact that the two-loop correction in Equation (45) is the square of the one-loop correction in Equation (46) qualitatively supports this expectation. However, it is an important open question to study the renormalization of the loop corrections in more detail.

5. Summary and Discussion

In this work, we have looked at the quantum corrections in the primordial power spectrum at two-loop orders in models of single-field inflation involving an intermediate USR phase engineered for PBH formation. This is the natural continuation of the previous works concerning the one-loop corrections. As the one-loop correction in models with sharp transition to the final SR phase can be large [1,11], it is necessary to examine the two-loop corrections for the severity of the loop contributions. As we have shown, there are eleven distinct one-particle irreducible Feynman diagrams at the two-loop orders. They require the cubic, quartic, quintic, and sextic interaction Hamiltonians.

As a first step forward, we have studied the corrections from the diagram (**a**) in Figure 1. This is because this diagram involves two vertices of quartic interaction, while their momentum integrals over q and k are separable. This brings computational simplicities. Other diagrams in Figure 1 are more complicated, either having higher-order nested integrals or the momentum integrals are not separable. On the other hand, the in-in analysis corresponding to diagram (**m**) would be easier to handle as it involves a single sextic Hamiltonian vertex. However, one has to calculate the action to a sixth order to construct $\mathbf{H_6}$, which involves additional technical complexities [81]. Our result shows that the two-loop corrections scale as the square of the one-loop corrections, i.e., like $\left(\Delta N e^{6\Delta N}\mathcal{P}_{\rm CMB}\right)^2$. This is interesting and physically expected. This result confirms the previous results [1,11] that the loop corrections can quickly lose control if the transition to the final attractor phase is very sharp and the duration of USR phase is long enough. In order for the loop corrections to be under perturbative control, and at the same time, to generate PBHs with the desired mass scales for dark matter purposes, it is necessary that the transition to the final attractor regime is mild so the loop corrections are rendered harmless.

The current work can be extended in various directions. One natural direction to proceed is to study the loop corrections from the remaining Feynman diagrams in Figure 1. While this is an interesting and yet cumbersome task, we believe that the total two-loop corrections would be similar to our current result, i.e., scaling like $\left(\Delta N e^{6\Delta N}\mathcal{P}_{\rm CMB}\right)^2$. The other direction to investigate is to study the general case of non-attractor inflation and the case of constant-roll inflation and see if the two-loop correction has a similar relation compared to the one-loop correction. Finally, an interesting direction to investigate is the question of regularization and renormalization at both one-loop and two-loop orders. We would like to come back to this important question in the future.

Funding: This work is supported partially by INSF of Iran under the grant number 4038049.

Data Availability Statement: No data are associated with this work.

Acknowledgments: We thank Jacopo Fumagalli, Haidar Sheikhahmadi, Amin Nassiri-Rad and Bahar Nikbakht for useful discussions. We thank ICCUB, University of Barcelona, for the kind hospitality during the workshop "BBH initiative: I. Primordial Black Holes" where this work was in progress.

Conflicts of Interest: The author declares no conflict of interest.

Appendix A. In-In Integrals

In this Appendix, we present the details of in-in analysis.

As explained in the main text, the two-loop corrections have the following contributions:

$$\langle\hat{O}(\tau_0)\rangle = \langle\hat{O}\rangle_{A_4A_4} + \langle\hat{O}\rangle_{A_4B_4} + \langle\hat{O}\rangle_{B_4A_4} + \langle\hat{O}\rangle_{B_4B_4}\,. \tag{A1}$$

In the main text, we have presented the results for $\langle\hat{O}\rangle_{A_4A_4}$, which we report here as well for concreteness:

$$\langle\hat{O}\rangle_{A_4A_4} = \int_{-\infty}^{\tau_0} d\tau_2 \int_{-\infty}^{\tau_2} d\tau_1 A_4(\tau_1)A_4(\tau_2) \int d^3\mathbf{x} \int d^3\mathbf{y} \Big\langle \Big[\mathcal{R}^2\mathcal{R}'^2(\mathbf{x},\tau_1), \big[\hat{O}(\tau_0), \mathcal{R}^2\mathcal{R}'^2(\mathbf{y},\tau_2)\big]\Big]\Big\rangle\,. \tag{A2}$$

Proceeding to the Fourier space, and after performing the contractions and imposing the constraints from the delta functions, in the soft limit where $p \ll q, k$, we obtain

$$\left\langle \mathcal{R}_{\mathbf{p}_1}\mathcal{R}_{\mathbf{p}_2}(\tau_0)\right\rangle_{A_4A_4} = (2\pi)^3\delta^3(\mathbf{p}_1+\mathbf{p}_2)\int_{-\infty}^{\tau_0} d\tau_2 \int_{-\infty}^{\tau_2} d\tau_1 A_4(\tau_1)A_4(\tau_2)\int \frac{d^3\mathbf{q}}{(2\pi)^3}\int \frac{d^3\mathbf{k}}{(2\pi)^3}F(\tau_1,\tau_2;k,q),$$

in which the function $F(\tau_1,\tau_2;k,q)$ has the following nine contributions:

$$\begin{aligned}
(a_0) &: (-4)(2)^2\mathrm{Im}\left[\mathcal{R}_p(\tau_0)^2\mathcal{R}_p^*(\tau_2)^2\right]\mathrm{Im}\left[\mathcal{R}_k{}'(\tau_1)^2\mathcal{R}_k'^*(\tau_2)^2\right]|\mathcal{R}_q(\tau_1)|^2\\
(b_0) &: (-4)(2)^2\mathrm{Im}\left[\mathcal{R}_p(\tau_0)^2\mathcal{R}_p^*(\tau_2)^2\right]\mathrm{Im}\left[\mathcal{R}_k(\tau_1)^2\mathcal{R}_k'^*(\tau_2)^2\right]|\mathcal{R}'_q(\tau_1)|^2\\
(c_0) &: (-4)(2)^3\mathrm{Im}\left[\mathcal{R}_p(\tau_0)^2\mathcal{R}_p^*(\tau_2)^2\right]\mathrm{Im}\left[\mathcal{R}_k(\tau_1)\mathcal{R}_k{}'(\tau_1)\mathcal{R}_k'^*(\tau_2)^2\right]\mathrm{Re}\left[\mathcal{R}_q(\tau_1)\mathcal{R}'_q(\tau_1)^*\right],
\end{aligned} \tag{A3}$$

and

$$\begin{aligned}
(d_0) &: (-4)(2)^4\mathrm{Im}\left[\mathcal{R}_p(\tau_0)^2\mathcal{R}_p^*(\tau_2)\mathcal{R}_p'^*(\tau_2)\right]\mathrm{Im}\left[\mathcal{R}_k{}'(\tau_1)^2\mathcal{R}_k'^*(\tau_2)\mathcal{R}_k^*(\tau_2)\right]|\mathcal{R}_q(\tau_1)|^2\\
(e_0) &: (-4)(2)^4\mathrm{Im}\left[\mathcal{R}_p(\tau_0)^2\mathcal{R}_p^*(\tau_2)\mathcal{R}_p'^*(\tau_2)\right]\mathrm{Im}\left[\mathcal{R}_k(\tau_1)^2\mathcal{R}_k'^*(\tau_2)\mathcal{R}_k^*(\tau_2)\right]|\mathcal{R}'_q(\tau_1)|^2\\
(f_0) &: (-4)(2)^5\mathrm{Im}\left[\mathcal{R}_p(\tau_0)^2\mathcal{R}_p^*(\tau_2)\mathcal{R}_p'^*(\tau_2)\right]\mathrm{Im}\left[\mathcal{R}_k(\tau_1)\mathcal{R}_k{}'(\tau_1)\mathcal{R}_k'^*(\tau_2)\mathcal{R}_k^*(\tau_2)\right]\mathrm{Re}\left[\mathcal{R}_q(\tau_1)\mathcal{R}'_q(\tau_1)^*\right],
\end{aligned} \tag{A4}$$

and

$$\begin{aligned}
(m) &: (-4)(2)^2\mathrm{Im}\left[\mathcal{R}_p(\tau_0)^2\mathcal{R}_p'^*(\tau_2)^2\right]\mathrm{Im}\left[\mathcal{R}_k{}'(\tau_1)^2\mathcal{R}_k^*(\tau_2)^2\right]|\mathcal{R}_q(\tau_1)|^2,\\
(n) &: (-4)(2)^2\mathrm{Im}\left[\mathcal{R}_p(\tau_0)^2\mathcal{R}_p'^*(\tau_2)^2\right]\mathrm{Im}\left[\mathcal{R}_k(\tau_1)^2\mathcal{R}_k^*(\tau_2)^2\right]|\mathcal{R}'_q(\tau_1)|^2,\\
(r) &: (-4)(2)^3\mathrm{Im}\left[\mathcal{R}_p(\tau_0)^2\mathcal{R}_p'^*(\tau_2)^2\right]\mathrm{Im}\left[\mathcal{R}_k(\tau_1)\mathcal{R}_k{}'(\tau_1)\mathcal{R}_k^*(\tau_2)^2\right]\mathrm{Re}\left[\mathcal{R}_q(\tau_1)\mathcal{R}'_q(\tau_1)^*\right].
\end{aligned} \tag{A5}$$

Now, we consider the contribution $\langle\hat{O}\rangle_{A_4B_4}$, yielding

$$\begin{aligned}
\langle\hat{O}\rangle_{A_4B_4} = &\int_{-\infty}^{\tau_0} d\tau_2\int_{-\infty}^{\tau_2} d\tau_1 A_4(\tau_1)B_4(\tau_2)\Big[\prod_i^4\int\frac{d^3\mathbf{q}_i}{(2\pi)^3}(2\pi)^3\delta^3(\sum_i\mathbf{q}_i)\Big]\Big[\prod_j^4\int\frac{d^3\mathbf{k}_i}{(2\pi)^3}(2\pi)^3\delta^3(\sum_i\mathbf{k}_i)\Big]\\
&\times\left\langle\Big[(\hat{\mathcal{R}}_{\mathbf{q}_1}\hat{\mathcal{R}}_{\mathbf{q}_2}\hat{\mathcal{R}}'_{\mathbf{q}_3}\hat{\mathcal{R}}'_{\mathbf{q}_4})(\tau_1),\Big[(\hat{\mathcal{R}}_{\mathbf{p}_1}\hat{\mathcal{R}}_{\mathbf{p}_2})(\tau_0),(\hat{\mathcal{R}}_{\mathbf{k}_1}\hat{\mathcal{R}}_{\mathbf{k}_2}\hat{\mathcal{R}}_{\mathbf{k}_3}\hat{\mathcal{R}}_{\mathbf{k}_4})(\tau_2)\Big]\Big]\right\rangle i^2\mathbf{k}_3\cdot\mathbf{k}_4\,.
\end{aligned} \tag{A6}$$

The leading contributions are those in which $\hat{\mathcal{R}}_{\mathbf{p}}(\tau_0)$ does not contract with $\hat{\mathcal{R}}_{\mathbf{k}_3}(\tau_2)$ and $\hat{\mathcal{R}}_{\mathbf{k}_4}(\tau_2)$. Correspondingly, the leading terms will be similar to terms (a_0), (b_0), and (c_0) in the analysis of $\langle\hat{O}\rangle_{A_4A_4}$. More specifically, the leading terms are

$$\begin{aligned}
(a_1) &: (-4)(2)^2\mathrm{Im}\left[\mathcal{R}_p(\tau_0)^2\mathcal{R}_p^*(\tau_2)^2\right]\mathrm{Im}\left[\mathcal{R}_k{}'(\tau_1)^2\mathcal{R}_k^*(\tau_2)^2\right]|\mathcal{R}_q(\tau_1)|^2(-i^2k^2)\\
(b_1) &: (-4)(2)^2\mathrm{Im}\left[\mathcal{R}_p(\tau_0)^2\mathcal{R}_p^*(\tau_2)^2\right]\mathrm{Im}\left[\mathcal{R}_k(\tau_1)^2\mathcal{R}_k^*(\tau_2)^2\right]|\mathcal{R}'_q(\tau_1)|^2(-i^2k^2)\\
(c_1) &: (-4)(2)^3\mathrm{Im}\left[\mathcal{R}_p(\tau_0)^2\mathcal{R}_p^*(\tau_2)^2\right]\mathrm{Im}\left[\mathcal{R}_k(\tau_1)\mathcal{R}_k{}'(\tau_1)\mathcal{R}_k^*(\tau_2)^2\right]\mathrm{Re}\left[\mathcal{R}_q(\tau_1)\mathcal{R}'_q(\tau_1)^*\right](-i^2k^2).
\end{aligned} \tag{A7}$$

Now consider $\langle\hat{O}\rangle_{B_4A_4}$, yielding,

$$\begin{aligned}
\langle\hat{O}\rangle_{B_4A_4} = &\int_{-\infty}^{\tau_0} d\tau_2\int_{-\infty}^{\tau_2} d\tau_1 B_4(\tau_1)A_4(\tau_2)\Big[\prod_i^4\int\frac{d^3\mathbf{q}_i}{(2\pi)^3}(2\pi)^3\delta^3(\sum_i\mathbf{q}_i)\Big]\Big[\prod_j^4\int\frac{d^3\mathbf{k}_i}{(2\pi)^3}(2\pi)^3\delta^3(\sum_i\mathbf{k}_i)\Big]\\
&\times\left\langle\Big[(\hat{\mathcal{R}}_{\mathbf{q}_1}\hat{\mathcal{R}}_{\mathbf{q}_2}\hat{\mathcal{R}}_{\mathbf{q}_3}\hat{\mathcal{R}}_{\mathbf{q}_4})(\tau_1),\Big[(\hat{\mathcal{R}}_{\mathbf{p}_1}\hat{\mathcal{R}}_{\mathbf{p}_2})(\tau_0),(\hat{\mathcal{R}}_{\mathbf{k}_1}\hat{\mathcal{R}}_{\mathbf{k}_2}\hat{\mathcal{R}}'_{\mathbf{k}_3}\hat{\mathcal{R}}'_{\mathbf{k}_4})(\tau_2)\Big]\Big]\right\rangle i^2\mathbf{q}_3\cdot\mathbf{q}_4\,.
\end{aligned} \tag{A8}$$

The leading contributions are (a_0), (b_0), (c_0), (d_0), (e_0), and (f_0) in $\langle\hat{O}\rangle_{A_4A_4}$, yielding

$$\begin{aligned}
(a_2) &: (-4)(2)^2\mathrm{Im}\big[\mathcal{R}_p(\tau_0)^2\mathcal{R}_p^*(\tau_2)^2\big]\mathrm{Im}\big[\mathcal{R}_k(\tau_1)^2\mathcal{R}_k'^*(\tau_2)^2\big]|\mathcal{R}_q(\tau_1)|^2(-i^2k^2)\\
(b_2) &: (-4)(2)^2\mathrm{Im}\big[\mathcal{R}_p(\tau_0)^2\mathcal{R}_p^*(\tau_2)^2\big]\mathrm{Im}\big[\mathcal{R}_k(\tau_1)^2\mathcal{R}_k'^*(\tau_2)^2\big]|\mathcal{R}_q(\tau_1)|^2(-i^2q^2)\\
(c_2) &: (-4)(2)^4\mathrm{Im}\big[\mathcal{R}_p(\tau_0)^2\mathcal{R}_p^*(\tau_2)^2\big]\mathrm{Im}\big[\mathcal{R}_k(\tau_1)^2\mathcal{R}_k'^*(\tau_2)^2\big]|\mathcal{R}_q(\tau_1)|^2(i^2\mathbf{k}\cdot\mathbf{q})
\end{aligned} \tag{A9}$$

and

$$\begin{aligned}
(d_2) &: (-4)(2)^4\mathrm{Im}\big[\mathcal{R}_p(\tau_0)^2\mathcal{R}_p^*(\tau_2)\mathcal{R}_p'^*(\tau_2)\big]\mathrm{Im}\big[\mathcal{R}_k(\tau_1)^2\mathcal{R}_k'^*(\tau_2)\mathcal{R}_k^*(\tau_2)\big]|\mathcal{R}_q(\tau_1)|^2(-i^2k^2)\\
(e_2) &: (-4)(2)^4\mathrm{Im}\big[\mathcal{R}_p(\tau_0)^2\mathcal{R}_p^*(\tau_2)\mathcal{R}_p'^*(\tau_2)\big]\mathrm{Im}\big[\mathcal{R}_k(\tau_1)^2\mathcal{R}_k'^*(\tau_2)\mathcal{R}_k^*(\tau_2)\big]|\mathcal{R}_q(\tau_1)|^2(-i^2q^2)\\
(f_2) &: (-4)(2)^6\mathrm{Im}\big[\mathcal{R}_p(\tau_0)^2\mathcal{R}_p^*(\tau_2)\mathcal{R}_p'^*(\tau_2)\big]\mathrm{Im}\big[\mathcal{R}_k(\tau_1)^2\mathcal{R}_k'^*(\tau_2)\mathcal{R}_k^*(\tau_2)\big]\mathcal{R}_q(\tau_1)|^2(i^2\mathbf{k}\cdot\mathbf{q})
\end{aligned} \tag{A10}$$

From the six terms above, one can check that the terms (c_2) and (f_2) make zero contributions after performing the double momentum integrals of the form $\int d^3\mathbf{q}\, d^3\mathbf{k}\,(\mathbf{q}\cdot\mathbf{k})\mathcal{F}(\tau_1,\tau_2;k,q)$, which vanishes.

Finally, considering $\langle\hat{O}\rangle_{B_4B_4}$, we have

$$\begin{aligned}
\langle\hat{O}\rangle_{B_4B_4} = &\int_{-\infty}^{\tau_0} d\tau_2\int_{-\infty}^{\tau_2} d\tau_1 B_4(\tau_1)B_4(\tau_2)\Big[\prod_i^4\int\frac{d^3\mathbf{q}_i}{(2\pi)^3}(2\pi)^3\delta^3(\sum_i\mathbf{q}_i)\Big]\Big[\prod_j^4\int\frac{d^3\mathbf{k}_i}{(2\pi)^3}(2\pi)^3\delta^3(\sum_i\mathbf{k}_i)\Big]\\
&\times\Big\langle\Big[(\hat{\mathcal{R}}_{\mathbf{q}_1}\hat{\mathcal{R}}_{\mathbf{q}_2}\hat{\mathcal{R}}_{\mathbf{q}_3}\hat{\mathcal{R}}_{\mathbf{q}_4})(\tau_1),\Big[(\hat{\mathcal{R}}_{\mathbf{p}_1}\hat{\mathcal{R}}_{\mathbf{p}_2})(\tau_0),(\hat{\mathcal{R}}_{\mathbf{k}_1}\hat{\mathcal{R}}_{\mathbf{k}_2}\hat{\mathcal{R}}_{\mathbf{k}_3}\hat{\mathcal{R}}_{\mathbf{k}_4})(\tau_2)\Big]\Big]\Big\rangle(\mathbf{q}_3\cdot\mathbf{q}_4)(\mathbf{k}_3\cdot\mathbf{k}_4)\,.
\end{aligned} \tag{A11}$$

The leading contributions are the (a_0) and (b_0) terms, yielding

$$\begin{aligned}
(a_3) &: (-4)(2)^2\mathrm{Im}\big[\mathcal{R}_p(\tau_0)^2\mathcal{R}_p^*(\tau_2)^2\big]\mathrm{Im}\big[\mathcal{R}_k(\tau_1)^2\mathcal{R}_k^*(\tau_2)^2\big]|\mathcal{R}_q(\tau_1)|^2(-i^2k^2)^2\\
(b_3) &: (-4)(2)^2\mathrm{Im}\big[\mathcal{R}_p(\tau_0)^2\mathcal{R}_p^*(\tau_2)^2\big]\mathrm{Im}\big[\mathcal{R}_k(\tau_1)^2\mathcal{R}_k^*(\tau_2)^2\big]|\mathcal{R}_q(\tau_1)|^2(-i^2k^2)(-i^2q^2)
\end{aligned} \tag{A12}$$

So, in total, we have 15 leading terms (i.e., containing p^{-3}) given by (a_0), (b_0), (c_0), (d_0), (e_0), (f_0), (a_1), (b_1), (c_1), (a_2), (b_2), (d_2), (e_2), (a_3) and (b_3) listed above. Out of these 15 contributions, only the terms (b_0), (c_0), (d_0), (e_0), (f_0) scale as $\Delta N^2e^{12\Delta N}$, while the remaining terms scale like $\Delta Ne^{12\Delta N}$. In the limit of a large enough ΔN, we may neglect the latter contributions as the subleading corrections.

Calculating the leading terms from (b_0), (c_0), (d_0), (e_0), (f_0), and neglecting the common factor $(2\pi)^3\delta^3(\mathbf{p}_1+\mathbf{p}_2)$ and $\frac{(4\pi)^2}{(2\pi)^6}$ from the double azimuthal integrals over momentum, we obtain

$$(b_0) \;: \frac{27H^6}{512M_P^6\epsilon_i^3hp^3}(h^2+28h-384)\Delta N^2e^{12\Delta N}+\mathcal{O}(\Delta N)\,, \tag{A13}$$

$$(c_0) \;: \frac{-27H^6}{64M_P^6\epsilon_i^3hp^3}(h^2+8h+96)\Delta N^2e^{12\Delta N}+\mathcal{O}(\Delta N)\,, \tag{A14}$$

$$(d_0) \;: \frac{9H^6}{256M_P^6\epsilon_i^3hp^3}(h^2+8h+48)\Delta N^2e^{12\Delta N}+\mathcal{O}(\Delta N)\,, \tag{A15}$$

$$(e_0) \;: \frac{-9H^6}{256M_P^6\epsilon_i^3hp^3}(h^2+16h+96)\Delta N^2e^{12\Delta N}+\mathcal{O}(\Delta N)\,, \tag{A16}$$

$$(f_0) \;: \frac{-9H^6}{16M_P^6\epsilon_i^3hp^3}(h+6)\Delta N^2e^{12\Delta N}+\mathcal{O}(\Delta N)\,. \tag{A17}$$

In comparison, we also present the remaining ten subleading terms $(a_0), (a_1), ..., (b_3)$ as well:

$$(a_0) \quad : \frac{3H^6\Delta N e^{12\Delta N}}{5600M_P^6\epsilon_i^3 hp^3}(346h - 2997) + \mathcal{O}(\Delta N^0)\,, \tag{A18}$$

$$(a_1) \quad : \frac{H^6\Delta N e^{12\Delta N}}{206976000M_P^6\epsilon_i^3 hp^3}(808500h^2 + 51180091h - 44241120) + \mathcal{O}(\Delta N^0)\,, \tag{A19}$$

$$(b_1) \quad : \frac{3H^6\Delta N e^{12\Delta N}}{71680M_P^6\epsilon_i^3 hp^3}(1544h - 33024) + \mathcal{O}(\Delta N^0)\,, \tag{A20}$$

$$(c_1) \quad : \frac{3H^6\Delta N e^{12\Delta N}}{179200M_P^6\epsilon_i^3 hp^3}(2100h^2 + 82832h - 344832) + \mathcal{O}(\Delta N^0)\,, \tag{A21}$$

$$(a_2) \quad : \frac{H^6\Delta N e^{12\Delta N}}{5017600M_P^6\epsilon_i^3 hp^3}(78400h^2 + 1628972h - 21780864) + \mathcal{O}(\Delta N^0)\,, \tag{A22}$$

$$(b2) \quad : \frac{9H^6\Delta N e^{12\Delta N}}{17920M_P^6\epsilon_i^3 hp^3}(35h^2 - 246h - 10368) + \mathcal{O}(\Delta N^0)\,, \tag{A23}$$

$$(d2) \quad : \frac{3H^6\Delta N e^{12\Delta N}}{5017600M_P^6\epsilon_i^3 p^3}(4900h^2 - 162656h - 1374912) + \mathcal{O}(\Delta N^0)\,, \tag{A24}$$

$$(e2) \quad : \frac{-3H^6\Delta N e^{12\Delta N}}{20070400M_P^6\epsilon_i^3 p^3}(4900h^2 - 178080h + 5806080) + \mathcal{O}(\Delta N^0)\,, \tag{A25}$$

$$(a3) \quad : \frac{H^6\Delta N e^{12\Delta N}}{3763200M_P^6\epsilon_i^3 p^3}(478062h - 3175200) + \mathcal{O}(\Delta N^0)\,, \tag{A26}$$

$$(b3) \quad : \frac{H^6\Delta N e^{12\Delta N}}{313600M_P^6\epsilon_i^3 p^3}(58637h - 423360) + \mathcal{O}(\Delta N^0)\,. \tag{A27}$$

Combining the five leading contributions $(b_0), (c_0), (d_0), (e_0), (f_0)$, and including all numerical factors, we obtain our final result:

$$\langle \mathcal{R}_{\mathbf{p}_1}\mathcal{R}_{\mathbf{p}_2}\rangle\big|_{2-\text{loops}} = (2\pi)^3\delta^3(\mathbf{p}_1+\mathbf{p}_2)\frac{-27H^6(4\pi)^2}{512M_P^6\epsilon_i^3 hp^3(2\pi)^6}(23h^2+132h+1152)\Delta N^2 e^{12\Delta N} + \mathcal{O}(\Delta N)\,.$$

Now, multiplying by the factor $\frac{p^3}{2\pi^2}$ to construct the dimensionless power spectrum, we end up with our fractional two-loop correction as follows:

$$\frac{\Delta\mathcal{P}^{(2-\text{loop})}}{\mathcal{P}_{\text{CMB}}} \simeq -\frac{27(23h^2+132h+1152)}{8h}\, e^{12\Delta N}N^2\mathcal{P}_{\text{CMB}}^2 + \mathcal{O}(\Delta N)\,, \tag{A28}$$

where $\mathcal{P}_{\text{CMB}}$ is the tree-level power spectrum for the CMB scale modes given in Equation (44).

References

1. Kristiano, J.; Yokoyama, J. Constraining Primordial Black Hole Formation from Single-Field Inflation. *Phys. Rev. Lett.* **2024**, *132*, 221003. [CrossRef] [PubMed]
2. Kristiano, J.; Yokoyama, J. Note on the bispectrum and one-loop corrections in single-field inflation with primordial black hole formation. *Phys. Rev. D* **2024**, *109*, 103541. [CrossRef]
3. Riotto, A. The Primordial Black Hole Formation from Single-Field Inflation is Not Ruled Out. *arXiv* **2023**, arXiv:2301.00599.
4. Riotto, A. The Primordial Black Hole Formation from Single-Field Inflation is Still Not Ruled Out. *arXiv* **2023**, arXiv:2303.01727.
5. Choudhury, S.; Gangopadhyay, M.R.; Sami, M. No-go for the formation of heavy mass Primordial Black Holes in Single Field Inflation. *Eur. Phys. J. C* **2024**, *84*, 884. [CrossRef]
6. Choudhury, S.; Panda, S.; Sami, M. PBH formation in EFT of single field inflation with sharp transition. *Phys. Lett. B* **2023**, *845*, 138123. [CrossRef]
7. Choudhury, S.; Panda, S.; Sami, M. Quantum loop effects on the power spectrum and constraints on primordial black holes. *J. Cosmol. Astropart. Phys.* **2023**, *11*, 066. [CrossRef]

8. Choudhury, S.; Panda, S.; Sami, M. Galileon inflation evades the no-go for PBH formation in the single-field framework. *J. Cosmol. Astropart. Phys.* **2023**, *8*, 078. [CrossRef]
9. Choudhury, S.; Karde, A.; Panda, S.; Sami, M. Realisation of the ultra-slow roll phase in Galileon inflation and PBH overproduction. *J. Cosmol. Astropart. Phys.* **2024**, *7*, 034. [CrossRef]
10. Choudhury, S.; Sami, M. Large fluctuations and Primordial Black Holes. *arXiv* **2024**, arXiv:2407.17006. [CrossRef]
11. Firouzjahi, H. One-loop corrections in power spectrum in single field inflation. *J. Cosmol. Astropart. Phys.* **2023**, *10*, 006. [CrossRef]
12. Motohashi, H.; Tada, Y. Squeezed bispectrum and one-loop corrections in transient constant-roll inflation. *J. Cosmol. Astropart. Phys.* **2023**, *8*, 069. [CrossRef]
13. Firouzjahi, H.; Riotto, A. Primordial Black Holes and loops in single-field inflation. *J. Cosmol. Astropart. Phys.* **2024**, *2*, 021. [CrossRef]
14. Tasinato, G. Large $|\eta|$ approach to single field inflation. *Phys. Rev. D* **2023**, *108*, 043526. [CrossRef]
15. Franciolini, G.; Iovino, A.J.; Taoso, M.; Urbano, A. Perturbativity in the presence of ultraslow-roll dynamics. *Phys. Rev. D* **2024**, *109*, 123550. [CrossRef]
16. Firouzjahi, H. Loop corrections in gravitational wave spectrum in single field inflation. *Phys. Rev. D* **2023**, *108*, 043532. [CrossRef]
17. Maity, S.; Ragavendra, H.V.; Sethi, S.K.; Sriramkumar, L. Loop contributions to the scalar power spectrum due to quartic order action in ultra slow roll inflation. *J. Cosmol. Astropart. Phys.* **2024**, *5*, 046. [CrossRef]
18. Cheng, S.L.; Lee, D.S.; Ng, K.W. Primordial perturbations from ultra-slow-roll single-field inflation with quantum loop effects. *J. Cosmol. Astropart. Phys.* **2024**, *3*, 008. [CrossRef]
19. Fumagalli, J.; Bhattacharya, S.; Peloso, M.; Renaux-Petel, S.; Witkowski, L.T. One-loop infrared rescattering by enhanced scalar fluctuations during inflation. *J. Cosmol. Astropart. Phys.* **2024**, *4*, 029. [CrossRef]
20. Nassiri-Rad, A.; Asadi, K. Induced gravitational waves from non-attractor inflation and NANOGrav data. *J. Cosmol. Astropart. Phys.* **2024**, *4*, 009. [CrossRef]
21. Meng, D.S.; Yuan, C.; Huang, Q.G. One-loop correction to the enhanced curvature perturbation with local-type non-Gaussianity for the formation of primordial black holes. *Phys. Rev. D* **2022**, *106*, 063508. [CrossRef]
22. Cheng, S.L.; Lee, D.S.; Ng, K.W. Power spectrum of primordial perturbations during ultra-slow-roll inflation with back reaction effects. *Phys. Lett. B* **2022**, *827*, 136956. [CrossRef]
23. Fumagalli, J. Absence of one-loop effects on large scales from small scales in non-slow-roll dynamics. *arXiv* **2023**, arXiv:2305.19263.
24. Tada, Y.; Terada, T.; Tokuda, J. Cancellation of quantum corrections on the soft curvature perturbations. *J. High Energy Phys.* **2024**, *1*, 105. [CrossRef]
25. Firouzjahi, H. Revisiting loop corrections in single field ultraslow-roll inflation. *Phys. Rev. D* **2024**, *109*, 043514. [CrossRef]
26. Iacconi, L.; Mulryne, D.J. Multi-field inflation with large scalar fluctuations: Non-Gaussianity and perturbativity. *J. Cosmol. Astropart. Phys.* **2023**, *9*, 033. [CrossRef]
27. Davies, M.W.; Iacconi, L.; Mulryne, D.J. Numerical 1-loop correction from a potential yielding ultra-slow-roll dynamics. *J. Cosmol. Astropart. Phys.* **2024**, *4*, 050. [CrossRef]
28. Iacconi, L.; Mulryne, D.; Seery, D. Loop corrections in the separate universe picture. *J. Cosmol. Astropart. Phys.* **2024**, *6*, 062. [CrossRef]
29. Kristiano, J.; Yokoyama, J. Comparing sharp and smooth transitions of the second slow-roll parameter in single-field inflation. *J. Cosmol. Astropart. Phys.* **2024**, *10*, 036. [CrossRef]
30. Kristiano, J.; Yokoyama, J. Generating large primordial fluctuations in single-field inflation for PBH formation. *arXiv* **2024**, arXiv:2405.12149.
31. Ballesteros, G.; Egea, J.G. One-loop power spectrum in ultra slow-roll inflation and implications for primordial black hole dark matter. *J. Cosmol. Astropart. Phys.* **2024**, *7*, 052. [CrossRef]
32. Kawaguchi, R.; Tsujikawa, S.; Yamada, Y. Roles of boundary and equation-of-motion terms in cosmological correlation functions. *Phys. Lett. B* **2024**, *856*, 138962. [CrossRef]
33. Braglia, M.; Pinol, L. No time to derive: Unraveling total time derivatives in in-in perturbation theory. *J. High Energy Phys.* **2024**, *8*, 068. [CrossRef]
34. Firouzjahi, H. Loop corrections in the bispectrum in ultraslow-roll inflation with PBHs formation. *Phys. Rev. D* **2024**, *110*, 043519. [CrossRef]
35. Caravano, A.; Franciolini, G.; Renaux-Petel, S. Ultra-Slow-Roll Inflation on the Lattice: Backreaction and Nonlinear Effects. *arXiv* **2024**, arXiv:2410.23942.
36. Caravano, A.; Inomata, K.; Renaux-Petel, S. Inflationary Butterfly Effect: Nonperturbative Dynamics from Small-Scale Features. *Phys. Rev. Lett.* **2024**, *133*, 15. [CrossRef]
37. Saburov, S.; Ketov, S.V. Quantum Loop Corrections in the Modified Gravity Model of Starobinsky Inflation with Primordial Black Hole Production. *Universe* **2024**, *10*, 354. [CrossRef]
38. Seery, D. One-loop corrections to the curvature perturbation from inflation. *J. Cosmol. Astropart. Phys.* **2008**, *2*, 006. [CrossRef]
39. Seery, D. One-loop corrections to a scalar field during inflation. *J. Cosmol. Astropart. Phys.* **2007**, *11*, 025. [CrossRef]
40. Senatore, L.; Zaldarriaga, M. On Loops in Inflation. *J. High Energy Phys.* **2010**, *12*, 008. [CrossRef]
41. Pimentel, G.L.; Senatore, L.; Zaldarriaga, M. On Loops in Inflation III: Time Independence of zeta in Single Clock Inflation. *J. High Energy Phys.* **2012**, *7*, 166. [CrossRef]

42. Inomata, K.; Braglia, M.; Chen, X.; Renaux-Petel, S. Questions on calculation of primordial power spectrum with large spikes: The resonance model case. *J. Cosmol. Astropart. Phys.* **2023**, *4*, 011; Erratum in *J. Cosmol. Astropart. Phys.* **2023**, *9*, E01. [CrossRef]
43. Ivanov, P.; Naselsky, P.; Novikov, I. Inflation and primordial black holes as dark matter. *Phys. Rev. D* **1994**, *50*, 7173–7178. [CrossRef] [PubMed]
44. Garcia-Bellido, J.; Morales, E.R. Primordial black holes from single field models of inflation. *Phys. Dark Univ.* **2017**, *18*, 47–54. [CrossRef]
45. Germani, C.; Prokopec, T. On primordial black holes from an inflection point. *Phys. Dark Univ.* **2017**, *18*, 6–10. [CrossRef]
46. Biagetti, M.; Franciolini, G.; Kehagias, A.; Riotto, A. Primordial Black Holes from Inflation and Quantum Diffusion. *J. Cosmol. Astropart. Phys.* **2018**, *7*, 032. [CrossRef]
47. Khlopov, M.Y. Primordial Black Holes. *Res. Astron. Astrophys.* **2010**, *10*, 495–528. [CrossRef]
48. Özsoy, O.; Tasinato, G. Inflation and Primordial Black Holes. *Universe* **2023**, *9*, 203. [CrossRef]
49. Byrnes, C.T.; Cole, P.S. Lecture notes on inflation and primordial black holes. *arXiv* **2021**, arXiv:2112.05716.
50. Escrivà, A.; Kuhnel, F.; Tada, Y. Primordial Black Holes. *arXiv* **2022**, arXiv:2211.05767. [CrossRef]
51. Pi, S. Non-Gaussianities in primordial black hole formation and induced gravitational waves. *arXiv* **2024**, arXiv:2404.06151.
52. Maldacena, J.M. Non-Gaussian features of primordial fluctuations in single field inflationary models. *J. High Energy Phys.* **2003**, *305*, 013. [CrossRef]
53. Jarnhus, P.R.; Sloth, M.S. de Sitter limit of inflation and nonlinear perturbation theory. *J. Cosmol. Astropart. Phys.* **2008**, *2*, 013. [CrossRef]
54. Arroja, F.; Koyama, K. Non-gaussianity from the trispectrum in general single field inflation. *Phys. Rev. D* **2008**, *77*, 083517. [CrossRef]
55. Inomata, K. Superhorizon Curvature Perturbations Are Protected against One-Loop Corrections. *Phys. Rev. Lett.* **2024**, *133*, 141001. [CrossRef] [PubMed]
56. Kawaguchi, R.; Tsujikawa, S.; Yamada, Y. Proving the absence of large one-loop corrections to the power spectrum of curvature perturbations in transient ultra-slow-roll inflation within the path-integral approach. *arXiv* **2024**, arXiv:2407.19742. [CrossRef]
57. Fumagalli, J. Absence of one-loop effects on large scales from small scales in non-slow-roll dynamics II: Quartic interactions and consistency relations. *arXiv* **2024**, arXiv:2408.08296.
58. Kinney, W.H. Horizon crossing and inflation with large eta. *Phys. Rev. D* **2005**, *72*, 023515. [CrossRef]
59. Namjoo, M.H.; Firouzjahi, H.; Sasaki, M. Violation of non-Gaussianity consistency relation in a single field inflationary model. *Europhys. Lett.* **2013**, *101*, 39001. [CrossRef]
60. Martin, J.; Motohashi, H.; Suyama, T. Ultra Slow-Roll Inflation and the non-Gaussianity Consistency Relation. *Phys. Rev. D* **2013**, *87*, 023514. [CrossRef]
61. Chen, X.; Firouzjahi, H.; Namjoo, M.H.; Sasaki, M. A Single Field Inflation Model with Large Local Non-Gaussianity. *Europhys. Lett.* **2013**, *102*, 59001. [CrossRef]
62. Morse, M.J.P.; Kinney, W.H. Large-η constant-roll inflation is never an attractor. *Phys. Rev. D* **2018**, *97*, 123519. [CrossRef]
63. Lin, W.C.; Morse, M.J.P.; Kinney, W.H. Dynamical Analysis of Attractor Behavior in Constant Roll Inflation. *J. Cosmol. Astropart. Phys.* **2019**, *9*, 063. [CrossRef]
64. Dimopoulos, K. Ultra slow-roll inflation demystified. *Phys. Lett. B* **2017**, *775*, 262–265. [CrossRef]
65. Chen, X.; Firouzjahi, H.; Komatsu, E.; Namjoo, M.H.; Sasaki, M. In-in and δN calculations of the bispectrum from non-attractor single-field inflation. *J. Cosmol. Astropart. Phys.* **2013**, *1312*, 039. [CrossRef]
66. Akhshik, M.; Firouzjahi, H.; Jazayeri, S. Effective Field Theory of non-Attractor Inflation. *J. Cosmol. Astropart. Phys.* **2015**, *7*, 048. [CrossRef]
67. Akhshik, M.; Firouzjahi, H.; Jazayeri, S. Cosmological Perturbations and the Weinberg Theorem. *J. Cosmol. Astropart. Phys.* **2015**, *12*, 027. [CrossRef]
68. Mooij, S.; Palma, G.A. Consistently violating the non-Gaussian consistency relation. *J. Cosmol. Astropart. Phys.* **2015**, *11*, 025. [CrossRef]
69. Bravo, R.; Mooij, S.; Palma, G.A.; Pradenas, B. A generalized non-Gaussian consistency relation for single field inflation. *J. Cosmol. Astropart. Phys.* **2018**, *5*, 024. [CrossRef]
70. Finelli, B.; Goon, G.; Pajer, E.; Santoni, L. Soft Theorems For Shift-Symmetric Cosmologies. *Phys. Rev. D* **2018**, *97*, 063531. [CrossRef]
71. Passaglia, S.; Hu, W.; Motohashi, H. Primordial black holes and local non-Gaussianity in canonical inflation. *Phys. Rev. D* **2019**, *99*, 043536. [CrossRef]
72. Pi, S.; Sasaki, M. Logarithmic Duality of the Curvature Perturbation. *Phys. Rev. Lett.* **2023**, *131*, 011002. [CrossRef]
73. Özsoy, O.; Tasinato, G. Consistency conditions and primordial black holes in single field inflation. *Phys. Rev. D* **2022**, *105*, 023524. [CrossRef]
74. Firouzjahi, H.; Riotto, A. Sign of non-Gaussianity and the primordial black holes abundance. *Phys. Rev. D* **2023**, *108*, 123504. [CrossRef]
75. Namjoo, M.H. One consistency relation for all single-field inflationary models. *J. Cosmol. Astropart. Phys.* **2024**, *5*, 041. [CrossRef]
76. Namjoo, M.H.; Nikbakht, B. Non-Gaussianity consistency relations and their consequences for the peaks. *J. Cosmol. Astropart. Phys.* **2024**, *8*, 005. [CrossRef]

77. Cai, Y.F.; Chen, X.; Namjoo, M.H.; Sasaki, M.; Wang, D.G.; Wang, Z. Revisiting non-Gaussianity from non-attractor inflation models. *J. Cosmol. Astropart. Phys.* **2018**, *5*, 012. [CrossRef]
78. Weinberg, S. *The Quantum Theory of Fields*; Volume 1: Foundations; Cambridge University Press: Cambridge, UK, 2005. [CrossRef]
79. Cheung, C.; Creminelli, P.; Fitzpatrick, A.L.; Kaplan, J.; Senatore, L. The Effective Field Theory of Inflation. *J. High Energy Phys.* **2008**, *803*, 014. [CrossRef]
80. Cheung, C.; Fitzpatrick, A.L.; Kaplan, J.; Senatore, L. On the consistency relation of the 3-point function in single field inflation. *J. Cosmol. Astropart. Phys.* **2008**, *802*, 021. [CrossRef]
81. Hassan Firouzjahi and Bahar Nikbakht, *in progress*.
82. Chen, X.; Huang, M.X.; Shiu, G. The Inflationary Trispectrum for Models with Large Non-Gaussianities. *Phys. Rev. D* **2006**, *74*, 121301. [CrossRef]
83. Chen, X.; Hu, B.; Huang, M.X.; Shiu, G.; Wang, Y. Large Primordial Trispectra in General Single Field Inflation. *J. Cosmol. Astropart. Phys.* **2009**, *8*, 008. [CrossRef]
84. Weinberg, S. Quantum contributions to cosmological correlations. *Phys. Rev. D* **2005**, *72*, 043514. [CrossRef]